

Analyzing Oscillators using Describing Functions

Tianshi Wang

Department of EECS, University of California, Berkeley, CA, USA

Email: tianshi@berkeley.edu

Abstract

In this manuscript, we discuss the use of describing functions as a systematic approach to the analysis and design of oscillators. Describing functions are traditionally used to study the stability of nonlinear control systems, and have been adapted for analyzing LC oscillators. We show that they can be applied to other categories of oscillators too, including relaxation and ring oscillators. With the help of several examples of oscillators from various physical domains, we illustrate the techniques involved, and also demonstrate the effectiveness and limitations of describing functions for oscillator analysis.

I. Introduction

Oscillators can be found in virtually every area of science and technology. They are widely used in radio communication [1], clock generation [2], and even logic computation in both Boolean [3–6] and non-Boolean [7–9] paradigms. The design and use of oscillators are not limited to electronic ones. Integrated MEMS oscillators are designed with an aim of replacing traditional quartz crystal ones as on-chip frequency references [10–12]; spin torque oscillators are studied for potential RF applications [13–15]; chemical reaction oscillators work as clocks in synthetic biology [16, 17]; lasers are optical oscillators with a wide range of applications. The growing importance of oscillators in circuits and systems calls for a systematic design methodology for oscillators which is independent from physical domains. However, such an approach is still lacking. While structured design methodologies are available for oscillators with negative-feedback amplifiers [18, 19], different types of oscillators are still analyzed with vastly different methodologies. The fundamental design specifications, such as signal waveforms and frequency tuning range, *etc.*, are all calculated using separate models; the interconnections between them can be easily overlooked during design, causing the iterations and time to increase. Partly as a result of this lack of structured study, researchers in domains other than electronics are often not aware of the similarity between their oscillators and some of the existing electronic ones. So instead of applying the existing models developed in electronics, they often rely heavily on experiments to guide their design, leading to higher design costs as well as less optimal results.

In this manuscript, we use describing function analysis to study oscillators in a systematic way. Describing function analysis has been practically applied to nonlinear control system design for many decades [20]. It is a general approach for analyzing the stability as well as predicting limit cycle properties such as frequency and amplitude of nonlinear systems. It generates graphical results in the complex plane that can provide system designers with convenient visualization for analyzing oscillation and exploring design margins. It is an immediate and natural candidate for studying oscillators in a systematic way. And in fact, it has been successfully applied to oscillator design previously [21, 22]. However, these works focus mainly on negative-resistance-feedback LC oscillators in the electronic domain. Ring oscillators are never part of the scope. Neither are relaxation oscillators, especially when the amplifier inside has non-negligible delays. Overall, the use of describing function in the

context of general domain-independent oscillator design still warrants discussion; examples from oscillators in different physical domains are highly needed.

We start the manuscript by providing the readers with essential background knowledge of describing function analysis in the context of nonlinear control theory in Sec. II. Then we use the analysis to study three common categories of oscillators: negative-resistance-feedback LC oscillators, relaxation oscillators and ring oscillators in Sec. III. Examples from electronics, biology and neuroscience are used as demonstration. In the meanwhile, we also address the limitations of describing function method and provide thoughts on potential improvements on it for oscillator design. Furthermore, in Sec. IV, we explore the use of describing function in the design of oscillators. In particular, we redesign a relaxation oscillator to make its response more like a harmonic oscillator in Section Sec. IV-A. We show that despite differences in their physical implementations, relaxation and harmonic LC oscillators can be treated as the same type of oscillators from describing function analysis' point of view, and they share the same mathematical equations. Conclusions and further research plans are provided in Section Sec. V.

II. Background

In this section we provide background knowledge of describing function analysis in the context of nonlinear control theory.

A. What are describing functions?

Given a general nonlinear algebraic function $y = f(x)$, without being concerned with its physical interpretation or application, we can define and derive its describing function in the following manner:

- 1) set $x(A, t) = A \cdot \sin(\omega t)$ as the input to $f(x)$, $x(A, t)$ is periodical in t with period $2\pi/\omega$;
- 2) get output: $y(A, t) = f(x(A, t)) = f(A \cdot \sin(\omega t))$, $y(A, t)$ is also periodical in t with period $2\pi/\omega$;
- 3) Fourier transform $y(A, t)$, get Fourier coefficient $Y(A)$ at fundamental frequency $\omega/2\pi$;
- 4) define the describing function of $y = f(x)$ as $N(A) = Y(A)/A$.

Mathematically, we can write $N(A)$ as

$$N(A) = \frac{1}{A}(a_1 + j \cdot b_1), \quad (1)$$

where

$$a_1 = +\frac{1}{\pi} \int_0^{2\pi} f(A \cdot \sin(\omega t)) \sin(\omega t) d\omega t, \quad (2)$$

$$b_1 = -\frac{1}{\pi} \int_0^{2\pi} f(A \cdot \sin(\omega t)) \cos(\omega t) d\omega t. \quad (3)$$

Note that the choice of ω doesn't affect the value of $N(A)$ as $f(x)$ is a memoryless algebraic function. This can be explained in (2) and (3). When we consider ωt as a single variable, the values of the integrals don't rely on the choice of the notation of this variable.

Graphically, the definition of $N(A)$ can be illustrated as in Figure 1. With sinusoidal input $x(A, t) = A \cdot \sin(\omega t)$, $Y(A)$ can be viewed as the amplitude of the sinusoidal wave at the fundamental frequency of the output. In this way, the describing function can be intuitively thought of as the frequency domain linear approximation of the nonlinear algebraic function that transfers an input phasor (sinusoidal wave) with amplitude A to an output phasor $Y(A) = A \cdot N(A)$.

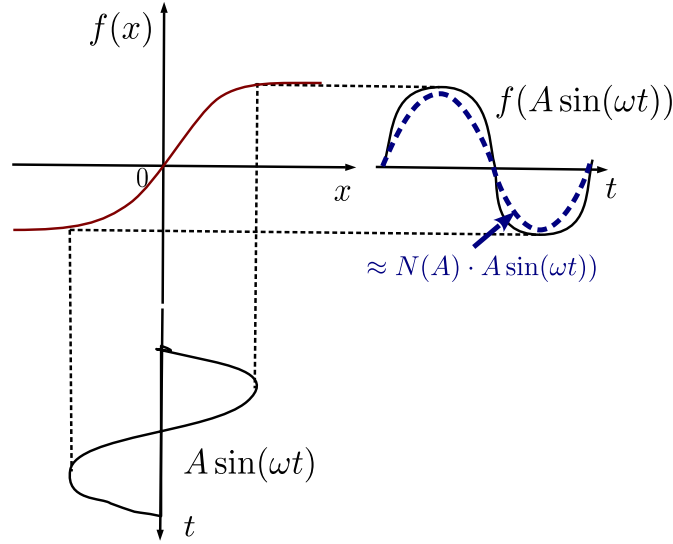


Fig. 1: Plot illustrating the definition of describing function.

B. How to calculate describing functions?

The definition of describing function as in (1), (2) and (3) provides a direct method for its calculation. Analytically calculated describing functions for some nonlinear functions common in control systems are listed in Table I. Take the ideal saturation characteristic function as shown in Table I No. 1 as an example:

$$f(x) = \begin{cases} -K \cdot a & \text{if } x \leq -a \\ K \cdot x & \text{if } -a < x < a \\ K \cdot a & \text{if } x \geq +a. \end{cases} \quad (4)$$

With input $x(A, t) = A \cdot \sin(\omega t)$, output $y(A, t)$ is

$$y(A, t) = \begin{cases} Ka & \text{if } 2k\pi + \Phi < \omega t < (2k+1)\pi - \Phi \\ -Ka & \text{if } (2k+1)\pi + \Phi < \omega t < (2k+2)\pi - \Phi \\ KA \sin(\omega t) & \text{everywhere else,} \end{cases} \quad (5)$$

where $k \in \mathbf{Z}$ and $\Phi = \arcsin(a/A)$, assuming $A \geq a$.

Now we calculate $N(A)$ analytically.

$$a_1 = \frac{1}{\pi} \int_0^{2\pi} f(A \cdot \sin(\omega t)) \sin(\omega t) d\omega t \quad (6)$$

$$= \frac{4}{\pi} \int_0^{\pi/2} f(A \cdot \sin(\omega t)) \sin(\omega t) d\omega t \quad (7)$$

$$= \frac{4}{\pi} \left[\int_0^{\Phi} KA \sin^2(\omega t) d\omega t + \int_{\Phi}^{\pi/2} Ka \sin(\omega t) d\omega t \right] \quad (8)$$

$$= \frac{2KA}{\pi} \left[\arcsin\left(\frac{a}{A}\right) + \frac{a}{A} \sqrt{1 - \left(\frac{a}{A}\right)^2} \right]. \quad (9)$$

Similarly, we have

$$b_1 = -\frac{1}{\pi} \int_0^{2\pi} f(A \cdot \sin(\omega t)) \cos(\omega t) d\omega t \quad (10)$$

$$\begin{aligned} &= -\frac{1}{\pi} \int_0^{\pi/2} f(A \cdot \sin(\omega t)) \cos(\omega t) d\omega t - \frac{1}{\pi} \int_{\pi/2}^{\pi} f(A \cdot \sin(\omega t)) \cos(\omega t) d\omega t \\ &\quad - \frac{1}{\pi} \int_{\pi}^{3\pi/2} f(A \cdot \sin(\omega t)) \cos(\omega t) d\omega t - \frac{1}{\pi} \int_{3\pi/2}^{2\pi} f(A \cdot \sin(\omega t)) \cos(\omega t) d\omega t. \end{aligned} \quad (11)$$

Because

$$\begin{aligned} &\frac{1}{\pi} \int_{\pi/2}^{\pi} f(A \cdot \sin(\omega t)) \cos(\omega t) d\omega t \\ &= \frac{1}{\pi} \int_{\pi/2}^0 f(A \cdot \sin(\pi - \omega t)) (-\cos(\pi - \omega t)) (-d(\pi - \omega t)) \end{aligned} \quad (12)$$

$$= -\frac{1}{\pi} \int_0^{\pi/2} f(A \cdot \sin(\theta)) \cos(\theta) d\theta, \quad (13)$$

where $\theta = \pi - \omega t$.

We have

$$\frac{1}{\pi} \int_0^{\pi/2} f(A \cdot \sin(\omega t)) \cos(\omega t) d\omega t + \frac{1}{\pi} \int_{\pi/2}^{\pi} f(A \cdot \sin(\omega t)) \cos(\omega t) d\omega t = 0, \quad (14)$$

and similarly

$$\frac{1}{\pi} \int_{\pi}^{3\pi/2} f(A \cdot \sin(\omega t)) \cos(\omega t) d\omega t + \frac{1}{\pi} \int_{3\pi/2}^{2\pi} f(A \cdot \sin(\omega t)) \cos(\omega t) d\omega t = 0. \quad (15)$$

Therefore

$$\implies b_1 = 0. \quad (16)$$

Finally the analytical expression of the describing function of ideal saturation function (4) can be calculated as

$$\begin{aligned} N(A) &= \frac{1}{A} (a_1 + j \cdot b_1) \\ &= \frac{2K}{\pi} \left[\arcsin\left(\frac{a}{A}\right) + \frac{a}{A} \sqrt{1 - \left(\frac{a}{A}\right)^2} \right], (A \geq a) \end{aligned} \quad (17)$$

Describing functions shown in Table I are calculated analytically in the same manner.

However, we may not always be able to express analytical integrals as in 2 and 3 explicitly. Alternative to the analytical calculation procedures, describing functions can also be calculated numerically just by sweeping A of the input, generating outputs through interpolation on tabulated data of $f(x)$, and performing Fourier transformation on the outputs to acquire the Fourier coefficients at the fundamental frequency.

C. How to use describing functions?

Describing function $N(A)$ of a nonlinear function in the loose sense transfers a sinusoidal wave with amplitude A to another sinusoidal wave with amplitude $|N(A) \cdot A|$ and phase $\angle(N(A))$. In this way, describing function $N(A)$ can be viewed as the frequency domain approximation of $f(x)$ that maps input phasor A to output phasor $N(A) \cdot A$. Note that when $f(X)$ is linear, analytical calculation shows that its describing function is constant regardless of input amplitude A . This is consistent with the frequency domain expression of one-port linear systems.

With describing functions acting as approximations to nonlinear functions, we can analyse general nonlinear systems in frequency domain and apply stability criteria that are available in linear control

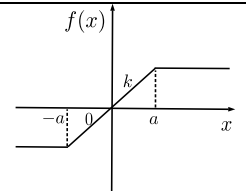
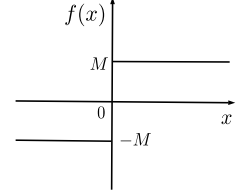
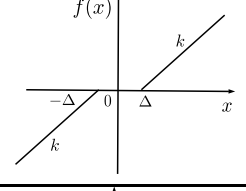
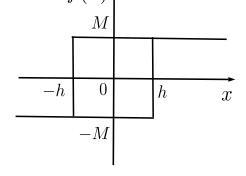
No.	Non-linearities	Describing Functions
1		$N(A) = \frac{2K}{\pi} \left[\arcsin\left(\frac{a}{A}\right) + \frac{a}{A} \sqrt{1 - \left(\frac{a}{A}\right)^2} \right], (A \geq a)$
2		$N(A) = \frac{4M}{\pi A}$
3		$N(A) = \frac{2K}{\pi} \left[\frac{\pi}{2} - \arcsin\left(\frac{\Delta}{A}\right) - \frac{\Delta}{A} \sqrt{1 - \left(\frac{\Delta}{A}\right)^2} \right], (A \geq \Delta)$
4		$N(A) = \frac{4M}{\pi A} \sqrt{1 - \left(\frac{h}{A}\right)^2} - j \frac{4Mh}{\pi A^2}, (A \geq h)$

TABLE I: Describing Functions for nonlinearities that are common in control theory.

theory.

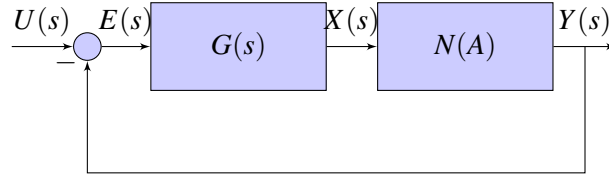


Fig. 2: A general nonlinear feedback system with separated one-port linear and nonlinear blocks.

Consider a nonlinear feedback system whose nonlinear and linear parts can be separated, as is show in Figure 2. Using describing function, we write its transfer function as:

$$H(s) = \frac{G(s) \cdot N(A)}{1 + G(s) \cdot N(A)} \quad (18)$$

This is a transfer function with a parameter A . At any given A , we can assess the stability of this system using Nyquist stability criterion. However, this lead to a common confusion of people new to describing function analysis: if $N(A)$ is only a valid approximation when the input and output of $f(x)$ are both sinusoidal with certain amplitudes, what does it mean when we say a system is stable or unstable?

Describing function analysis first assumes the system is already oscillating and periodical waveforms present everywhere in the system are all sinusoidal. With a given A , we further assumes the oscillating

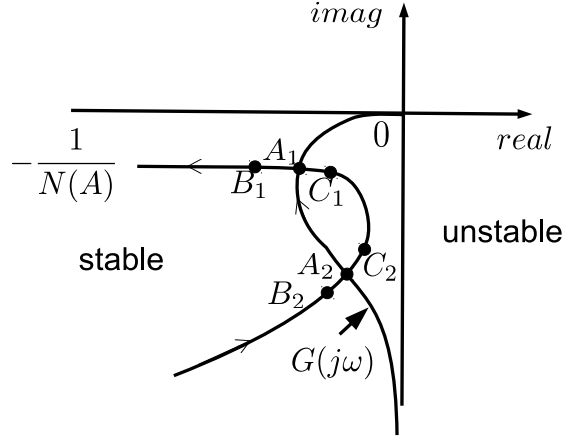


Fig. 3: Nyquist plot of $G(j\omega)$ intersected with $-\frac{1}{N(A)}$. Arrows on $G(j\omega)$ and $-\frac{1}{N(A)}$ indicate the increasing directions of ω and A respectively. When $-\frac{1}{N(A)}$ lands in area left of the Nyquist plot of $G(j\omega)$, the closed-loop system is stable. Two intersections are A_1 and A_2 .

waveform at the input of the nonlinear block has amplitude of A . Under all these assumptions, the transfer function in (18) holds well. Nyquist stability criterion is then applied to check whether the system is stable. If it is strictly stable (all closed-loop poles are in left-open plane) or strictly unstable, it indicates the assumptions we made are violated. Only when the system is marginally stable can there be chance for the system to actually oscillate at the assumed amplitude. The necessary condition for the system to be marginally stable is

$$-\frac{1}{N(A)} = G(s) \quad (19)$$

The condition (19) is satisfied when the plot of $-\frac{1}{N(A)}$ on complex plane graphically intersects with the Nyquist plot of $G(j\omega)$. And the ω and A with respect to the intersection provide predictions to the oscillation's frequency and amplitude (at the input of nonlinear block) respectively. As an example, in Figure 3 there are two intersections — A_1 and A_2 , indicating two possible oscillating operating points. Compared with other nonlinear system analyses like Harmonic Balance, describing function analysis not only locates possible oscillating operating points, but also provides information for the stability of oscillation. In Figure 3, if we assume that the system is oscillating at operating point A_1 . If there is some perturbation to the input of nonlinear block, A may change by a small amount. When A increases, A_1 shifts to B_1 ; the resulting closed-loop system becomes stable, causing A to decay and the operating point to move back to A_1 . When A decreases slightly to reach C_1 where the closed-loop system is unstable, A increases back to its value at the operating point A_1 . These observations indicate that the oscillation happening at intersection A_1 is stable. On the contrary, similar analysis predicts that oscillation at the other intersection A_2 is unstable, thus cannot be observed in the actual system.

III. Oscillator Analysis with Describing Functions

There are three main categories of oscillators: LC oscillators, ring oscillators and relaxation oscillators. In this section, we apply describing function analysis to all of them. In each category, we select typical examples, identify and separate linear and nonlinear parts of the systems, then apply describing function analysis to them and study its effectiveness and limitations.

A. LC Oscillators

Applying describing function analysis to negative-resistance-feedback LC oscillators is a natural choice, and has been studied before [21, 22]. In this section, we briefly go through the procedures and analyze an LC oscillator with a less common series RLC configuration, just to show the generality of the describing function analysis.

It is worth noting that a wide range of oscillators can be categorized as LC-type oscillators, including spin torque oscillators, MEMS oscillators, optical lasers, *etc.* The same analysis can be applied to all of them.

A schematic diagram of a series LC oscillator is given in the left-most plot in Figure 4. The negative resistor is usually nonlinear to ensure that the oscillation is amplitude-stable. To apply describing function analysis, we separate linear and nonlinear parts of the system as shown in the middle plot of Figure 4 and convert the system into block diagram.

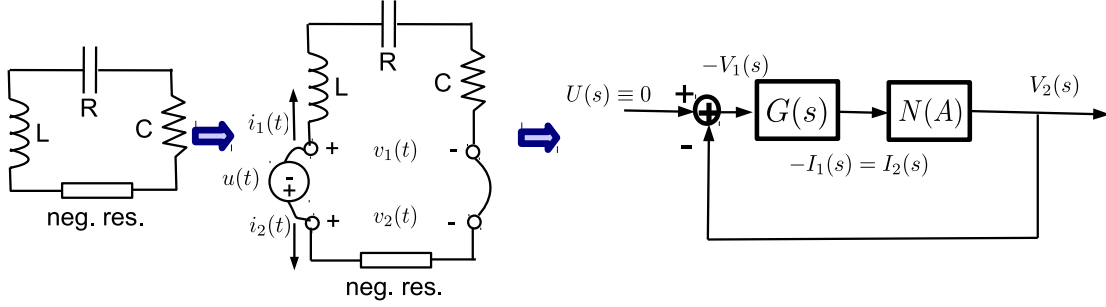


Fig. 4: Schematics and block diagram of a negative-resistance-feedback LC oscillator. The middle diagram shows how the series R-L-C-negative-resistor system is analyzed as a connection of nonlinear and linear parts.

In the block diagram in Figure 4:

$$G(s) = \frac{1}{R + \frac{1}{sC} + sL} = \frac{sC}{LC \cdot s^2 + RC \cdot s + 1}. \quad (20)$$

We can assume the negative nonlinear resistor has the following characteristic:

$$v_2 = f(i_2) = -V_{max} \cdot \tanh\left(\frac{R_{max}}{V_{max}} \cdot i_2\right). \quad (21)$$

The describing function of (21) can be acquired numerically by sweeping A in the sinusoidal input $i_2 = A \cdot \sin(\omega t)$. However, just to show a flavour of how describing functions can be calculated by hand in general, here we derive the describing function of (21) using Taylor expansion.

$$N(A) = \frac{1}{A\pi} \int_0^{2\pi} -V_{max} \cdot \tanh\left(\frac{R_{max}}{V_{max}} \cdot A \sin(\omega t)\right) \cdot \sin(\omega t) d(\omega t). \quad (22)$$

Because $\tanh(x) = x - \frac{1}{3}x^3 + \frac{2}{15}x^5 + o(x^5)$, we have

$$\begin{aligned} N(A) = & \frac{1}{A\pi} \int_0^{2\pi} -V_{max} \cdot \frac{AR_{max}}{V_{max}} \cdot \sin^2(\omega t) - \frac{1}{3} \frac{A^3 R_{max}^3}{V_{max}} \cdot \sin^4(\omega t) \\ & + \frac{2}{15} \frac{A^5 R_{max}^5}{V_{max}} \cdot \sin^6(\omega t) + o(\sin^6(\omega t)) d(\omega t). \end{aligned} \quad (23)$$

Using

$$\int \sin^2(x) dx = \frac{1}{2}(1 - \cos(2x)), \quad (24)$$

$$\int \sin^4(x) dx = \frac{1}{8}(3 - 4\cos(2x) + \cos(4x)), \quad (25)$$

$$\int \sin^6(x) dx = \frac{1}{32}(10 - 15\cos(2x) + 6\cos(4x) - \cos(6x)), \quad (26)$$

(23) is reduced to

$$N(A) = -R_{max} + \frac{R_{max}^3}{4V_{max}^2} \cdot A^2 - \frac{R_{max}^5}{12V_{max}^4} \cdot A^4 + o(A^4). \quad (27)$$

After characterizing the nonlinear block using describing function, we derive the transfer function of the system and the condition for it to oscillate. The transfer function is

$$H(s) = \frac{V_2(s)}{U(s)} = \frac{G(s) \cdot N(A)}{1 + G(s) \cdot N(A)}, \quad (28)$$

where $G(s)$ and $N(A)$ are given in (20) and (27) respectively. For the system to oscillate, $-1/N(A) = G(s)$ has to be satisfied. Given specific parameters, we will then be able to location the oscillation operating point of the system and predict the oscillation frequency as well as amplitudes of the waveforms.

B. Ring Oscillators

Ring oscillators are another type of oscillators that normally consist of odd numbers of inverters. The functionality of this type of oscillators relies on the delay each stage of inversion provides. Therefore, it is less obvious how memoryless nonlinearity can be separated from the system and how describing function analysis can be used. However, with some assumptions, describing function analysis can still be applied in this scenario.

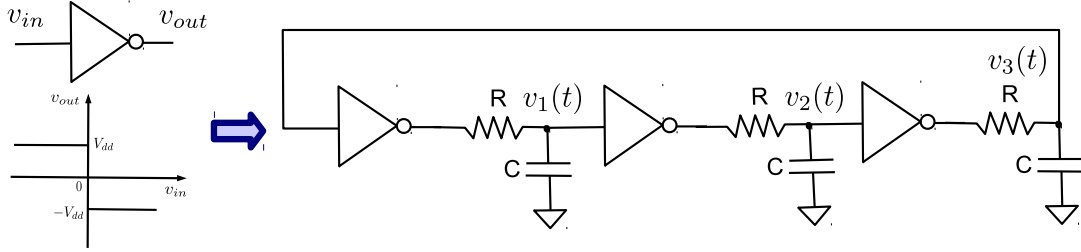


Fig. 5: 3-stage ring oscillator made of ideal inverters.

Figure 5 shows a three-stage ring oscillator made of inverters with an ideal inverse relay characteristics. It is common to assume that the three stages are identical, in both the inverter and the RC delay. The analytical solution for the oscillation frequency and amplitude of this system can be derived [23]:

$$A^* = \frac{\sqrt{5}-1}{2} \approx 0.618, \quad (29)$$

$$T^* = 6 \ln\left(\frac{1+\sqrt{5}}{2}\right) \cdot \tau \approx 2.89\tau, \quad (30)$$

where $\tau = RC$. V_{dd} is normalized to 1.

Now we apply describing function analysis to the system. We treat the first inverter (leftmost in Figure 5) as a memoryless nonlinearity. According to Table I, we know its describing function is

$$N(A) = -\frac{4V_{dd}}{\pi A} \quad (31)$$

The RC circuit can be easily modeled as a linear block. Since the stages are identical, the signals after the three stages are of the same waveforms with phases separated by $2\pi/3$. The waveform of $v_3(t)$ can be thought of as a time-delayed version of $v_1(t)$. Therefore, we can model the rest of the two stages as a pure time delay, which is a linear subsystem. This technique is illustrated in Figure 6. After these procedures, we can draw the block diagram of this ring oscillator as in Figure 7.

The transfer function derived from the block diagram in Figure 7 is

$$H(s) = \frac{V_3(s)}{U(s)} = \frac{G_2(s) \cdot G_1(s) \cdot N(A)}{1 - G_2(s) \cdot G_1(s) \cdot N(A)}, \quad (32)$$

where $N(A)$ is given in (31), $G_1(s)$ and $G_2(s)$ are

$$G_1(s) = \frac{1}{RC \cdot s + 1}, \quad G_2(s) = e^{-\frac{2}{3}Ts}. \quad (33)$$

For the system to oscillate, condition $1/N(A) = G_2(s) \cdot G_1(s)$ has to be satisfied. We can examine

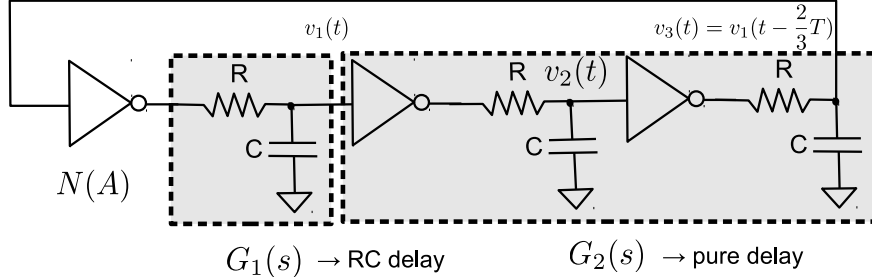


Fig. 6: Modelling the ring oscillator in Figure 5 by identifying nonlinear and linear blocks in the system.

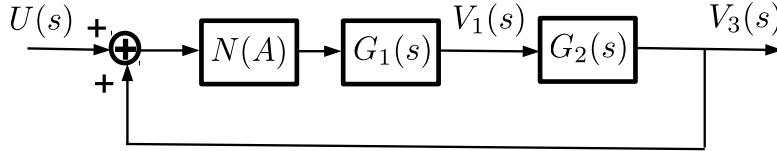


Fig. 7: Block diagram of the system in Figure 5.

this condition by overlaying the Nyquist plot of linear system $G_2(s) \cdot G_1(s)$ and the plot of $1/N(A)$ in the same complex plane in Figure 8.

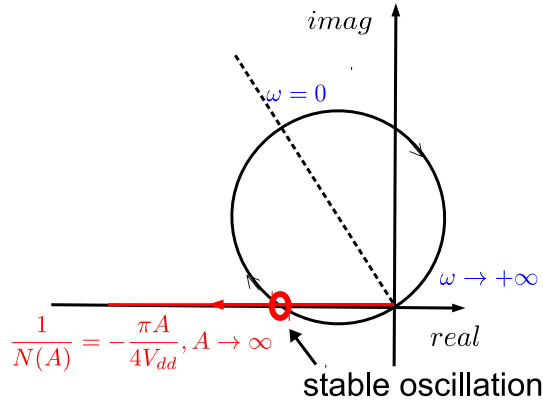


Fig. 8: Nyquist plot of $G_2(s) \cdot G_1(s)$ as in (33) and the plot of $1/N(A)$ as in (31) overlaid in the same complex plane. The intersection indicates a stable oscillating operating point.

Mathematically, the oscillation intersection in Figure 8 implies the following condition.

$$\frac{1}{N(A)} = G_2(j\omega) \cdot G_1(j\omega) = \frac{1}{RC \cdot j\omega + 1} e^{-j\frac{4\pi}{3}}. \quad (34)$$

From Figure 8 we observe that the intersection happens at $(-0.5, 0)$, which indicates $1/N(A) = -1/2$.

$$N(A) = -2 \implies -\frac{4V_{dd}}{\pi A} = -2 \implies A = \frac{2V_{dd}}{\pi} \approx 0.6366 \cdot V_{dd}. \quad (35)$$

When $V_{dd} = 1$, solution in (35) is 0.6366. It is reasonably close to the analytical solution 0.618 in (29).

To acquire the frequency of oscillation, we analyze the linear part of the system. At the intersection

in Figure 8,

$$G_2(j\omega) \cdot G_1(j\omega) = -0.5 \implies \left| \frac{1}{RC \cdot j\omega + 1} \right| = 0.5 \quad (36)$$

$$\implies RC \cdot |\omega| = \sqrt{3} \implies |\omega| = \frac{\sqrt{3}}{RC} \quad (37)$$

$$\implies T = \frac{2\pi}{\sqrt{3}} RC \approx 3.628\tau \quad (38)$$

Note that result in (38) is not so close to the analytical solution T^* in (30). This is mostly because in this example with ideal relay inverters, the oscillating waveforms are not close to being sinusoidal, so the results from describing function analysis are not guaranteed to be accurate. Nevertheless, an estimation can be acquired for the amplitude and frequency of the oscillation that are reasonably close to the analytical solutions.

In most cases, analytical solutions are not available, but describing function analysis is a general and systematic approach that can still be applied. Here, we consider changing the inverter to have more common and realistic nonlinear property such as

$$v_{out} = f(v_{in}) = -\hat{A} \tanh(k \cdot v_{in}). \quad (39)$$

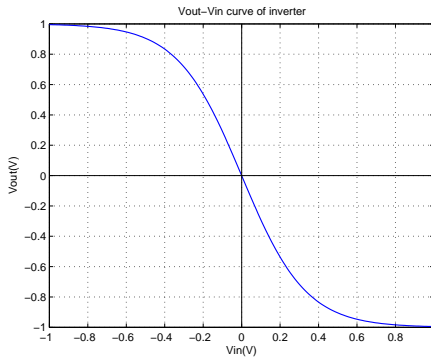
In this case it becomes difficult for analytical solutions to be derived. But the describing function of (39) can be easily calculated analytically or numerically. Just as in Section III-A, $N(A)$ can be approximated as

$$N(A) = -\hat{A}k + \frac{\hat{A}k^3}{4} \cdot A^2 - \frac{\hat{A}k^5}{12} \cdot A^4 + o(A^4) \quad (40)$$

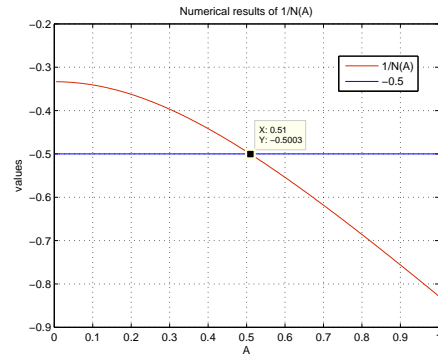
The block diagram of this ring oscillator is still unchanged from Figure 7. Nyquist plot of $G_2(s) \cdot G_1(s)$ overlaid with $1/N(A)$ is still the same of Figure 8 except that $N(A)$ is now given as (40). With parameters $\hat{A} = 1, k = 3$, we can calculate amplitude A at the intersection in Figure 8.

$$N(A) = -2 \implies -3 + \frac{3^3}{4} \cdot A^2 - \frac{3^5}{12} \cdot A^4 = -2 \implies A \approx \frac{2}{3}. \quad (41)$$

Since (40) turns out to be an inaccurate approximation to the describing function with $\tanh()$, we calculate the describing function numerically by sweeping A just to double check the result in (41). The inverter function as in (39) and the reciprocal of its describing function are plotted in Figure 9. From Figure 9(b) we observe that $1/N(A) = -0.5 \implies A \approx 0.51$. The linear part of this ring oscillator is unchanged from the one in Figure 7, so the solutions acquired from describing function analysis are $A \approx 0.51, T \approx 3.628\tau$.



(a) Plot of $V_{out} - V_{in}$ relationship as in (39).



(b) $1/N(A)$ vs. A .

Fig. 9: Plots of characteristics of the inverter as well as the reciprocal of its describing function.

We can test the results by performing numerical simulation on this 3-stage ring oscillator, and observe the transient simulation results shown in Figure 10. Measurements show that the amplitude of the input to the nonlinear block (e_{in1} in Figure 10) is 0.50 and the oscillation period of the system is around 3.5ms (with $\tau = 1ms$ in the circuit). These properties are quite accurately predicted by the describing function analysis. We emphasize again that in this example strict analytical solution is not available, making describing function analysis a valuable tool for providing predictions for ring oscillators.

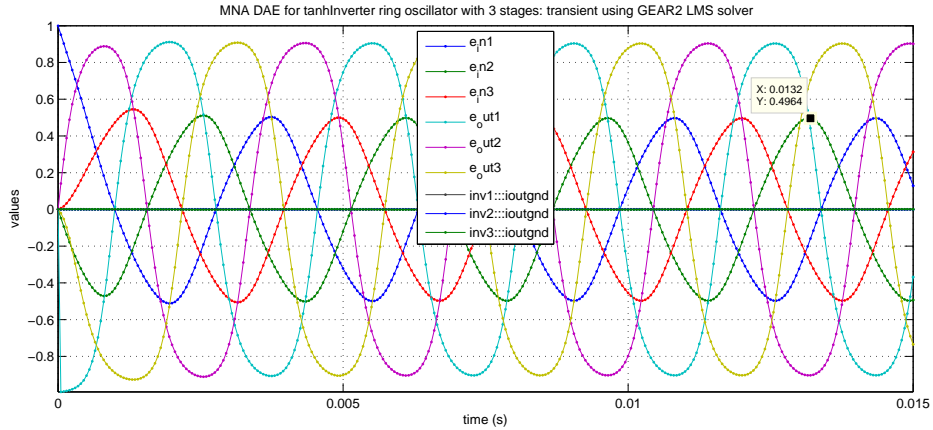


Fig. 10: Transient simulation results on system in Figure 5 with inverter characteristics described in (39).

Many oscillators can be categorized as ring oscillators too. One example is a synthetic biological ring oscillator — Elowitz Repressilator. Equations for each stage of Elowitz Repressilator can be written as

$$\frac{d}{dt}m_i = -m_i + \frac{\alpha}{1 + p_j^n} + \alpha_0 \quad (42)$$

$$\frac{d}{dt}p_i = -\beta(p_i - m_i) \quad (43)$$

Transient simulation results of Elowitz Repressilator with three stages are shown in Figure 11. In the simulation, we select parameters as $\alpha = 300$, $\alpha_0 = 0.03$, $n = 2$, and $\beta = 0.2$.

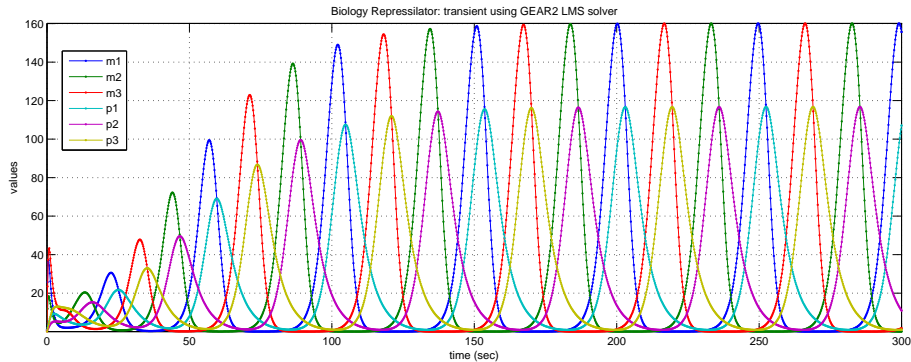


Fig. 11: Transient simulation results on Elowitz Repressilator system in (42) with (43)

Again, this system can be separated into nonlinear and linear blocks. Block diagram is the same as Figure 7 with linear and nonlinear parts:

$$G_1(s) = \frac{\beta}{s + \beta}, \quad G_2(s) = e^{-\frac{2}{3}Ts} \quad (44)$$

$$m = f(p) = \frac{\alpha}{1 + p^n} + \alpha_0 \quad (45)$$

Describing function analysis returns approximations to the oscillation amplitude and frequency — $T \approx 10/\beta$, $A \approx 40$. The frequency is rather accurate. The amplitude indicates that the swing is around 80, while in reality it is about 115. Unlike the nonlinearities studied before, function in (45) is not odd symmetric or centered at zero. So $A \sin(\omega t)$ is not a reasonable approximation to the input of this nonlinear block any more. In order to calculate the describing function of (45), offset of the oscillation has to be estimated. However, the relationship between this offset and the DC solution of the system is still not clear to the author. This limitation of the calculation of describing function requires further investigation.

C. Relaxation Oscillators

Relaxation oscillation often results from hysteresis. As is shown in the left plot of Figure 12, an electronic relaxation oscillator is often made by tying RC circuits to a Schmitt trigger in a feed-back loop. We can easily separate the nonlinear and linear blocks, then draw the system's block diagram as in the right plot of Figure 12. Based on the results in Table I, the describing function for ideal hysteresis can be written as

$$N(A) = \frac{4M}{\pi A} \sqrt{1 - \left(\frac{h}{A}\right)^2} - j \frac{4Mh}{\pi A^2}, \quad (A \geq h), \quad (46)$$

where M is the magnitude of nonlinear function $f(x)$ and $\pm h$ are the transition points for input x .

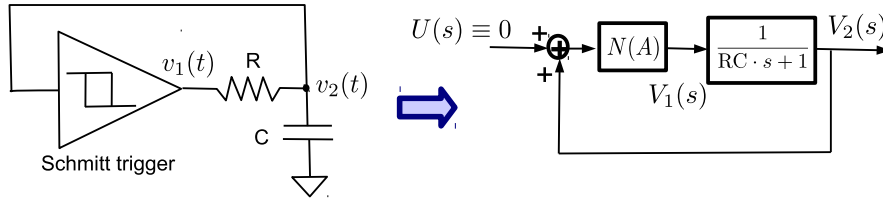


Fig. 12: Schematic and block diagram of the relaxation oscillator made of Schmitt trigger and RC circuit.

The transfer function from $U(s)$ to $V_2(s)$ is

$$H(s) = \frac{V_2(s)}{U(s)} = \frac{G(s) \cdot N(A)}{1 - G(s) \cdot N(A)} \quad (47)$$

When the system oscillates, $G(s) = 1/N(A)$ has to be satisfied. To observe the condition for oscillation more closely, we draw the Nyquist plot and $1/N(A)$ with different choice of parameters on the complex planes in Figure 13.

Using Nyquist stability criterion as discussed in Section II, we analyze the three scenarios shown in Figure 13. When $\pi h > 4M$ or $\pi h = 4M$, the system won't oscillate. When $\pi h < 4M$ there is one stable oscillation operating point. Oscillation frequency and amplitude can also be calculated from the plot in Figure 13 given all the design parameters.

However, properties of such an ideal relaxation oscillator calculated using describing function are difficult to be directly verified using simulation. This is because we modeled hysteresis directly as a memoryless nonlinearity while in fact the nature of hysteresis indicates the inevitable existence of some form of memory, and should instead be modelled with differential equations [24, 25].

To overcome this difficulty and model hysteresis in a more physical manner, we model a general

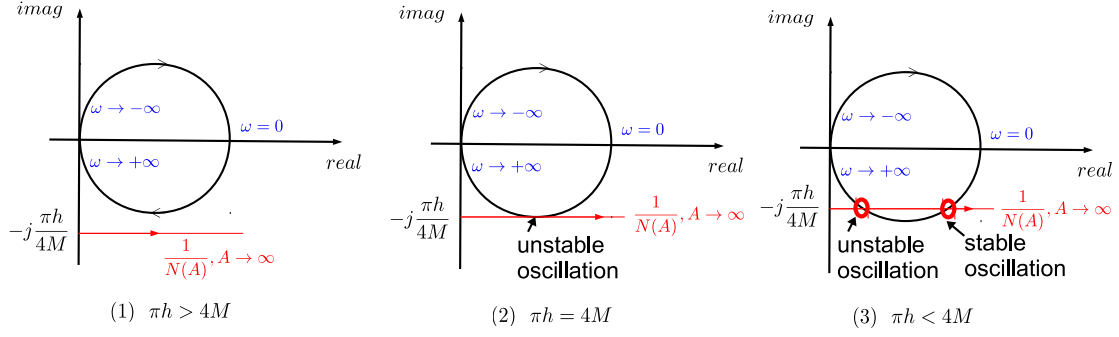


Fig. 13: Nyquist plot and the describing function of Schmitt trigger oscillator plotted on complex plane with conditions $\pi h > 4M$, $\pi h = 4M$ and $\pi h < 4M$.

relaxation oscillator using equations (48) and (49).

$$\tau_f \frac{d}{dt} v_o(t) = f(v_o(t)) - v_i(t) \triangleq \hat{v}_i(t) - v_i(t) \triangleq e(t), \quad (48)$$

$$\tau_s \frac{d}{dt} v_i(t) = v_o(t) - v_i(t). \quad (49)$$

We then directly convert the system described in (48) and (49) into block diagram and add auxiliary input $U(s)$, as in Figure 14.

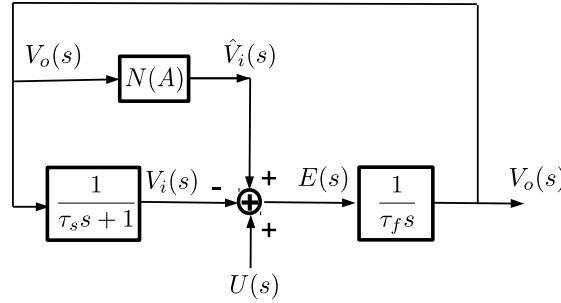


Fig. 14: Block diagram of the relaxation oscillator system as described in equations (48) and (49).

Figure 15 demonstrates the simplification procedures of the system through transformations on the block diagram in Figure 14. These simplification procedures are typical in control theory. After simplification, the nonlinear and linear blocks are separated and we are left with a simple system that is very similar to the system we studied in Section II.

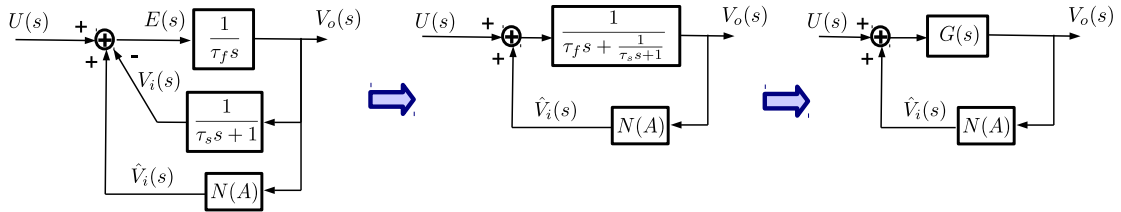


Fig. 15: Simplification of block diagram in Figure 14.

The transfer function of the resulting system is

$$H(s) = \frac{V_o(s)}{U(s)} = \frac{G(s)}{1 - N(A) \cdot G(s)} \quad (50)$$

where

$$G(s) = \frac{1}{\tau_f s + \frac{1}{\tau_s s + 1}}. \quad (51)$$

For the system to oscillate, $\frac{1}{N(A^*)} = G(j\omega)$ has to be satisfied. Here we choose our nonlinearity f as

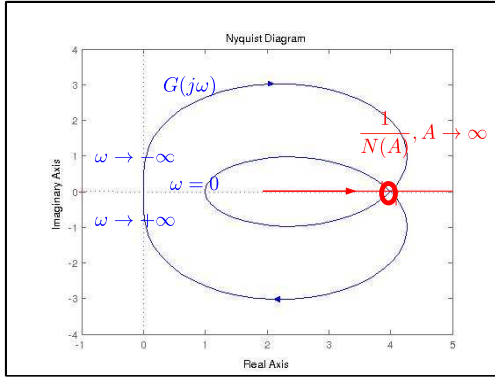
$$f(v_o) = -k_1 v_o + k_2 \cdot \tanh(k_3 v_o) \quad (52)$$

Analytical calculation result of the describing function of f (approximating \tanh using its Taylor expansion) is

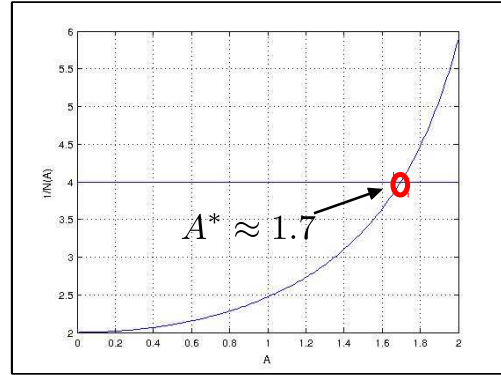
$$N(A) = \frac{1}{A\pi} \int_0^{2\pi} f(A \sin(\omega t)) \cdot \sin(\omega t) d\omega t \quad (53)$$

$$= -k_1 + k_2 k_3 - k_2 k_3^3 \cdot A^2 + \frac{1}{12} k_2 k_3^5 \cdot A^4 + o(A^4). \quad (54)$$

In order to analyze oscillation condition quantitatively, we select parameters: $\tau_f = 2.5 \times 10^{-4}$, $\tau_s = 1 \times 10^{-3}$, $k_1 = 2$, $k_2 = 2.5^2$, $k_3 = 1/2.5 = 0.4$. Then for the system to oscillate, $\frac{1}{N(A^*)} = G(j\omega) \implies \frac{1}{N(A^*)} = 4$. We then plot $\frac{1}{N(A)}$ in Figure 16(b) and observe that $\frac{1}{N(A^*)} = 4 \implies A^* \approx 1.7$.



(a) Nyquist plot of $G(s)$ as in (51) overlaid with $1/N(A)$.



(b) $1/N(A)$ vs. A .

Fig. 16: Nyquist plot and $1/N(A)$ plot of the relaxation oscillator in Figure 14.

The oscillation frequency can be predicted by looking at the intersection in Figure 16(a). For $G(j\omega)$ to intersect with real axis, $\angle G(j\omega)$ has to be equal to 0.

$$\angle G(j\omega) = \frac{1}{\tau_f \cdot j\omega + \frac{1}{\tau_s \cdot j\omega + 1}} = 0 \quad (55)$$

$$\implies (\tau_s - \tau_f)\omega - \tau_s \tau_f^2 \omega^3 = 0 \quad (56)$$

$$\implies \begin{cases} \omega_1 = 0 \\ \omega_{2,3} = \pm \frac{1}{\tau_s} \sqrt{\frac{\tau_s - \tau_f}{\tau_f}} \end{cases} \quad (57)$$

Substitute τ_s and τ_f in (57) with their values, we get the oscillation frequency $\omega^* \approx 1732$, or $f^* \approx 276\text{Hz}$.

Then we simulate the system in Figure 14 and plot the transient waveforms in Figure 17. From the waveforms we can see that the amplitude of the input to the nonlinear block is approximately 1.65

while the oscillation frequency is around 260Hz. These simulation results are close to our predictions acquired through describing function analysis.

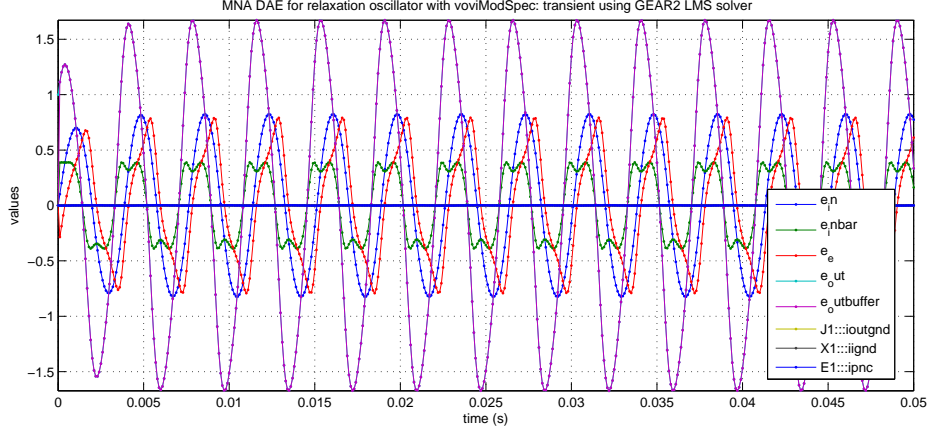


Fig. 17: Transient simulation results on system in Figure 14.

It is important to note that in the relaxation oscillator model in (48) and (49), we are not neglecting the delay from the nonlinear hysteretic component but instead consider both time constants τ_s and τ_f . Through the transformation of block diagrams, we have been able to separate the linear and nonlinear blocks in general for relaxation oscillators and apply describing function analysis effectively.

To further demonstrate the use of describing functions, we take a look at another example of relaxation oscillator from neural biology: Fitzhugh-Nagumo Neuron Model. The equations of the system can be written as:

$$\frac{d}{dt}v = v - \frac{v^3}{3} - w + I_{ext} \quad (58)$$

$$\tau \frac{d}{dt}w = v + a - bw \quad (59)$$

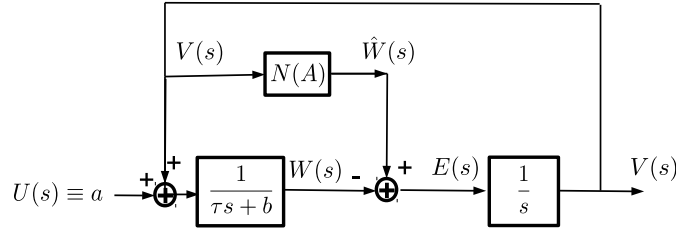


Fig. 18: Block diagram of the Fitzhugh-Nagumo neuron relaxation oscillator system.

Similar to the Schmitt-trigger-based electronic oscillator, this neuron system can also be expressed in block diagram format, as is shown in Figure 18, except that $N(A)$ here is the describing function of another f :

$$w = f(v) = v - \frac{v^3}{3} + I_{ext} \quad (60)$$

Its describing function is easy to derive analytically:

$$N(A) = 1 - \frac{3}{4}A^2. \quad (61)$$

Using similar simplification procedures to separate nonlinear and linear blocks and applying describing function analysis on the system, we will be able to predict stable oscillation phenomenon

for this neuron system given a set of parameters. For example, we select parameters $a = 0.7$, $b = 0.8$, $\tau = 12.5$, $I_{ext} = 0.5$. Transient simulation shows stable oscillation as in Figure 19. Describing function analysis can be applied in the same procedures as above, with $\tau_s = \tau$, $\tau_f = 1$. The Nyquist plot is of the same shape as Figure 16(a), but with the real axis intersection at ≈ 12.5 with $\omega \approx 0.25$. From the intersection we get $A^* \approx 1.1$ and $T^* \approx 25$. From transient results in Figure 19, we observe that the magnitude of v exceeds 1.1, and the oscillation period is close to 40. The results from describing function analysis is a little off in this example.

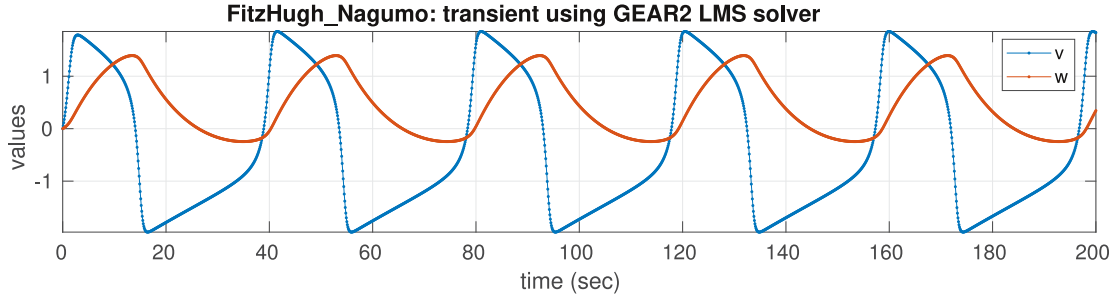


Fig. 19: Transient simulation results from Fitzhugh-Nagumo neuron relaxation oscillator.

It is worth mentioning that in the case of relaxation oscillators, the system waveforms are usually not sinusoidal, making the assumptions of describing function analysis inaccurate. In simulation, we have noticed that with well-separated τ_s and τ_f in the electronic relaxation oscillator system (48) and (49), the prediction of amplitude and frequency are not accurate. But even in this case, describing function analysis is usually still useful in predicting the occurrence of oscillation.

IV. Oscillator Design with Describing Functions

Knowledge gained from the analysis of oscillators can often shed light on the design procedures. Describing function analysis, with its graphical presentation of systems as well as its capability to separate systems into linear and nonlinear blocks with “orthogonal” functionalities, often provides useful insights into oscillator design. For example, the oscillation frequency involves only the linear block while the amplitude depends on the nonlinear one; the use of describing function allow designers to adjust them one by one. Apart from parameter adjusting, describing function also makes it easier for people to design oscillators from scratch. Just like designing negative-resistance LC oscillators, in MEMS [10–12] and spintronics [13–15] researchers often need to design circuitry around a linear resonator to make the oscillation self-sustaining. In these cases, describing function can also serve as a convenient tool.

In this section, we focus on one design example: making relaxation oscillators behave like a harmonic oscillator, which often indicates better energy efficiency and less distortion.

A. Design of “Harmonic” Relaxation Oscillators

We have studied relaxation oscillators in Section III-C. Here we look at the oscillator characterized in equations (48) and (49).

We have already converted the system in to block diagram Figure 14. Now we draw the Bode plot of the linear block in Figure 20.

Based on Figure 16(a) in Section III-C, oscillation happens at the location where $\angle G(j\omega_1) = 0$. Through calculation, we get the expression of ω_1 .

$$\omega_1 = \frac{1}{\tau_s} \sqrt{\frac{\tau_s - \tau_f}{\tau_f}} \quad (62)$$

For the waveforms to be more sinusoidal, the linear block should have the strongest filtering effect

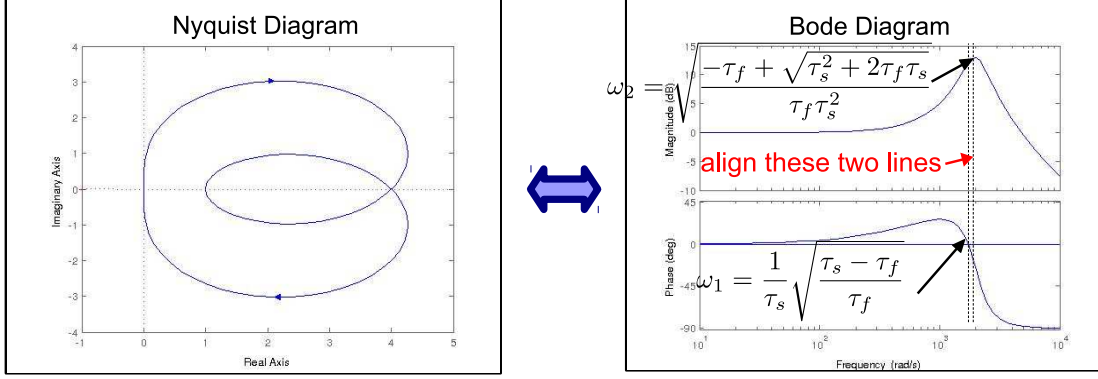


Fig. 20: Nyquist and Bode diagrams illustrating design ideas of for the linear block $G(s)$ to realize “harmonic-oscillator-like” relaxation oscillators.

around ω_1 . However, based on the Bode plot, the filtering effect is strongest when the magnitude of transfer function peaks. Assume it peaks at ω_2 , i.e. $\max\{|G(j\omega)|\} = |G(j\omega_2)|$.

$$\omega_2 = \sqrt{\frac{-\tau_f + \sqrt{\tau_s^2 + 2\tau_f\tau_s}}{\tau_f\tau_s^2}} \quad (63)$$

For ω_1 to be equal to ω_2 :

$$\sqrt{\frac{-\tau_f + \sqrt{\tau_s^2 + 2\tau_f\tau_s}}{\tau_f\tau_s^2}} = \frac{1}{\tau_s} \sqrt{\frac{\tau_s - \tau_f}{\tau_f}} \implies \tau_f = 0 \text{ or } \tau_s = 0 \quad (64)$$

(64) indicates under the system structure as in (48) and (49) ω_1 will never be equal to ω_2 . So instead, we observe the diagram Figure 14 and change the $1/(\tau_s s + 1)$ block to be $1/(\tau_s s + 1)$, and redraw the diagram in Figure 21. In this way, the transfer function of the linear block becomes

$$G(s) = \frac{1}{\tau_f s + \frac{1}{\tau_s s}} = \frac{\tau_s s}{\tau_f \tau_s s + 1} \quad (65)$$

Linear system in (65) has good filtering property so the resulting waveforms will become more sinusoidal.

It is worth mentioning that the (65) is essentially the equation of an LC tank. This indicates mathematically LC oscillators and relaxation oscillators are very similar.

To implement such a redesigned relaxation oscillator, instead of using RC circuit that results in $1/(\tau_s s + 1)$ block, we use integrator that can change the block transfer function to $1/(\tau_s s)$. The circuit schematic diagram is given in Figure 22.

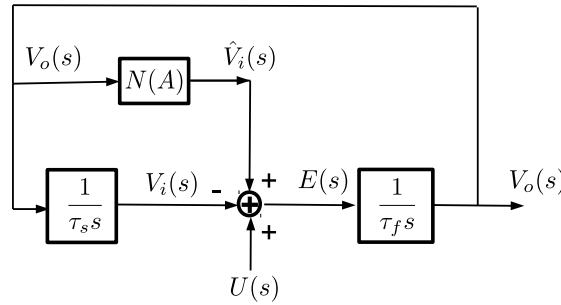


Fig. 21: Redesigned diagram of the relaxation oscillator as in Figure 14.

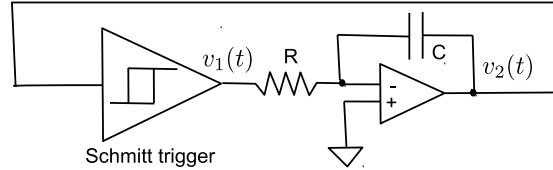


Fig. 22: Circuit implementation of the redesigned diagram in Figure 21.

V. Conclusions

In this manuscript, we studied different types of oscillators using the describing function analysis. We showed that the describing function analysis is a general, domain-independent, systematic approach to the study and design of oscillators. Examples used in this report demonstrated describing function analysis' effectiveness, but also revealed its limitations in its support for systems with non-sinusoidal waveforms. Such limitations can be overcome by adapting describing functions to incorporate higher-order harmonics. Also, describing functions with multiple inputs have potentials in analyzing multi-tone systems, shedding light on interesting properties such as injection locking and parametric oscillation. These are all part of our planned future work on the use of describing functions in oscillator analysis.

References

- [1] T. S. Rappaport and others. *Wireless Communications: Principles and Practice*, volume 2. Prentice Hall PTR New Jersey, 1996.
- [2] R. E. Best. *Phase locked loops: design, simulation, and applications*. McGraw-Hill Professional, 2007.
- [3] T. Wang and J. Roychowdhury. PHLOGON: PHase-based LOGic using Oscillatory Nanosystems. In *Proc. UCNC*, LNCS sublibrary: Theoretical computer science and general issues. Springer, July 2014. DOI link.
- [4] T. Wang and J. Roychowdhury. Design Tools for Oscillator-based Computing Systems. In *Proc. IEEE DAC*, pages 188:1–188:6, 2015. DOI link.
- [5] T. Wang and J. Roychowdhury. Oscillator-based Ising Machine, 2017.
- [6] T. Wang. Sub-harmonic Injection Locking in Metronomes. *arXiv preprint arXiv:1709.03886*, 2017.
- [7] F. Hoppensteadt and E. Izhikevich. Synchronization of laser oscillators, associative memory, and optical neurocomputing. *Physical Review E*, 62(3):4010, 2000.
- [8] P. Maffezzoni, B. Bahr, Z. Zhang and L. Daniel. Oscillator array models for associative memory and pattern recognition. *IEEE Trans. on Circuits and Systems I: Fundamental Theory and Applications*, 62(6):1591–1598, June 2015.
- [9] M. Pufall, W. Rippard, G. Csaba, D. Nikonov, G. Bourianoff and W. Porod. Physical Implementation of Coherently Coupled Oscillator Networks. *IEEE Journal on Exploratory Solid-State Computational Devices and Circuits*, 1:76–84, 2015.
- [10] L. Miri and H. Seyed. Design and Phase-noise Modeling of Temperature-compensated High Frequency MEMS-CMOS Reference Oscillators. 2010.
- [11] C. T.-C. Nguyen and R. T. Howe. An Integrated CMOS Micromechanical Resonator high-Q Oscillator. *IEEE Journal of Solid-State Circuits*.
- [12] C. T.-C. Nguyen. Micromechanical resonators for oscillators and filters. In *Proceedings of IEEE Ultrasonics Symposium*, volume 1, pages 489–499. IEEE, 1995.
- [13] D. Dixit, K. Konishi, C. V. Tomy, Y. Suzuki and A. A. Tulapurkar. Spintronic Oscillator based on Magnetic Field Feedback. *Applied Physics Letters*, 101(12):122410, 2012.
- [14] P. Villard, U. Ebels, D. Houssameddine, J. Katine, D. Mauri, B. Delaet, P. Vincent, M.-C. Cyrille, B. Viala, J.-P. Michel and others. A GHz Spintronic-based RF Oscillator. *IEEE Journal of Solid-State Circuits*, 45(1):214–223, 2010.
- [15] G. Finocchio, V. Puliafito, S. Komineas, L. Torres, O. Ozatay, T. Hauet and B. Azzerboni. Nanoscale Spintronic Oscillators based on the Excitation of Confined Soliton Modes. *Journal*

- of Applied Physics*, 114(16):163908, 2013.
- [16] T. Danino, O. Mondragón-Palomino, L. Tsimring and J. Hasty. A Synchronized Quorum of Genetic Clocks. *Nature*, 463(7279):326–330, 2010.
 - [17] M. Rosenblum and A. Pikovsky. Synchronization: from pendulum clocks to chaotic lasers and chemical oscillators. *Contemporary Physics*, 44(5):401–416, 2003.
 - [18] C. Verhoeven, S. A. Van, G. Monna, M. H. L. Kouwenhoven and E. Yildiz. *Structured Electronic Design: Negative-feedback Amplifiers*. Springer, 2010.
 - [19] A. Van Staveren, C. Verhoeven and A. van Roermund. *Structured Electronic Design: High-Performance Harmonic Oscillators and Bandgap References*. Springer, 2001.
 - [20] V. Vander and E. Wallace. *Multiple-input Describing Functions and Nonlinear System Design*. McGraw-Hill, 1968.
 - [21] J. Bank. *A Harmonic-oscillator Design Methodology based on Describing Functions*. Chalmers University of Technology, 2006.
 - [22] E. Vidal, A. Poveda and M. Ismail. Describing Functions and Oscillators. *Circuits and Devices Magazine*, 17(6):7–11, 2001.
 - [23] S. Srivastava and J. Roychowdhury. Analytical Equations for Nonlinear Phase Errors and Jitter in Ring Oscillators. *IEEE Transactions on Circuits and Systems*, 54(10):2321–2329, October 2007. DOI link.
 - [24] T. Wang and J. Roychowdhury. Well-Posed Models of Memristive Devices. *arXiv preprint arXiv:1605.04897*, 2016.
 - [25] T. Wang. Modelling Multistability and Hysteresis in ESD Clamps, Memristors and Other Devices. In *Proc. IEEE CICC*, pages 1–10. IEEE, 2017.